Original Article

Comparison of Strain Elastography, Shear Wave Elastography, and Conventional Ultrasound in Diagnosing Thyroid Nodules

CME Credits

Li-Jen Liao[1,2,3], Huan-Wen Chen[4], Wan-Lun Hsu[5], Yung-Sheng Chen[2]*

[1]Department of Otolaryngology, Far Eastern Memorial Hospital, New Taipei, Taiwan, [2]Department of Electrical Engineering, Yuan Ze University, Taoyuan, Taiwan, [3]Medical Engineering Office, Far Eastern Memorial Hospital, New Taipei, Taiwan, [4]Department of Internal Medicine, Lo-Hsu Medical Foundation, Lotung Poh-Ai Hospital, Yi-Lan, Taiwan, [5]Genomics Research Center, Academia Sinica, Taipei, Taiwan

Abstract

Objective: The purpose of this study is to compare the diagnostic performances of strain elastography (SE), shear wave elastography (SWE), and traditional ultrasound (US) features in diagnosing thyroid nodules. **Subjects and Methods:** This study included 185 adult patients with thyroid nodules who underwent conventional gray-scale US, SE, and SWE. SE was scored using a four-pattern elastographic scoring (ES) system. SWE values were presented as mean SWE values and standard derivation using Young's modules. The optimal cutoff values of the mean SWE values for predicting malignancy were determined using receiver operating characteristic (ROC) curve analysis. We used logistic regression models to test elastography as a novel significant predictor for the diagnosis of malignant nodules. The diagnostic performance of elastography parameters was compared with a traditional trained model. **Results:** Malignant thyroid nodules were stiffer for SE (ES patterns 1 and 2/3 and 4) and mean SWE values (4/17; 51.0 ± 24.4 kPa) than for benign nodules (114/50; 33.1 ± 25.2 kPa) ($P < 0.01$). In ROC curve analyses, a mean SWE value of 32 kPa was the optimal cutoff point, with diagnostic performance measures of 81% sensitivity, 65% specificity, a 23% positive predictive value (PPV), and 96% negative predictive value (NPV). In multivariate logistic regression, the mean SWE value (≥32 kPa) was an independent predictor for malignancy (odds ratio: 16.8; 95% confidence interval [CI]: 3.6–78.3). However, after the addition of SE and SWE to traditional US features, the C-statistic was not significantly increased compared to the traditional model (0.88, 95% CI: 0.81–0.94 vs. 0.91, 0.85–0.97, $P = 0.4$). **Conclusion:** In this study, we confirmed SWE as an independent predictor for malignant thyroid nodules. However, in comparing the new extended elastography model to our previous prediction model, the new extended model showed no significant difference in the diagnostic performance.

Keywords: Neck, real-time elastography, shear wave elastography, thyroid nodule, ultrasound

Introduction

Thyroid nodules are commonly found in the general population with a prevalence of approximately 4%–7% by palpation.[1] On ultrasound (US), the presence of thyroid nodules is found in 27%–67% of adults; thyroid nodules at autopsy are observed in nearly 30%–60% of the population.[2] Among the thyroid nodules in the general population, approximately 5%–12% are found to be malignant.[3,4] Several imaging modalities are used to assess thyroid nodules including computed tomography, magnetic resonance imaging, or US. Currently, US examination is the imaging method of choice for the differential diagnosis of thyroid nodules.

Initially, the decision for the management of thyroid nodules is made by comparing measurements of the nodular size over time with US. Many physicians refer patients with thyroid nodules to H and N surgeons for surgical treatment because of growth detection. Although US comparison of volume change is reasonable, it still has reliability variation because of different operators, tumor biologic variation, and US examination technique limitations.[5] Therefore, US-fine-needle aspiration (FNA) cytology is the prefer investigation of choice rather than for serial follow-up for a suspected malignant

Received: 31-03-2018 **Accepted:** 30-04-2018 **Available Online:** 06-06-2018

Access this article online

Quick Response Code:

Website: www.jmuonline.org

DOI: 10.4103/JMU.JMU_46_18

Address for correspondence: Prof. Yung -Sheng Chen, No.135, Yuan-Tung Road, Chung-Li 32003 Taiwan. E-mail: eeyschen@saturn.yzu.edu.tw

How to cite this article: Liao LJ, Chen HW, Hsu WL, Chen YS. Comparison of strain elastography, shear wave elastography, and conventional ultrasound in diagnosing thyroid nodules. J Med Ultrasound 2019;27:26-32.

thyroid nodule. In 2007, the National Cancer Institute recommended The Bethesda System for Reporting Thyroid Cytopathology (TBSRTC) because it has a high accuracy for determining thyroid cytopathology and guides further management of thyroid nodules.[6]

However, US-FNA remains an invasive procedure, and multiple nodules are commonly encountered; therefore, the most suspicious nodule is often selected for aspiration. Certain US characteristics can help in selecting thyroid nodes for US-FNA. Homogeneous thyroid nodules with well-defined regular margins often indicate benignity.[7] Other US findings suggestive of a malignant thyroid nodule include an irregular margin, microcalcification, hypoechogenicity, a taller-than-wide shape (an anterior-posterior diameter larger than the transverse diameter; AP/TR ratio ≥1), associated lymphadenopathy, and an intranodular vascular pattern.[8-10] However, no single criterion possesses both satisfactory sensitivity and specificity to diagnose malignant thyroid nodules. If we consider multiple US features and assume any suspicious US features as positive, we will increase sensitivity but decrease specificity. On the other hand, if we consider multiple suspicious US features simultaneously as positive, it will decrease the sensitivity and increase specificity. A scoring system integrating multiple US features could be more accurate than that of any single characteristic in predicting a malignant thyroid nodule.[11] We constructed a computerized scoring system in the US report system based on the sonographic findings for predicting a malignant thyroid nodule. Such a system could be beneficial in patient counseling and in providing physicians timely guidance on whether to conduct an US-FNA cytologic study for managing a controversial thyroid nodule. The prediction formula is combined with the following four B-mode US features: margin, microcalcification, echo-texture, and a taller-than-wide shape. This scoring model has been incorporated in a hospital-based reporting reminder system and is also freely shared on a website.[12]

Elastography is a promising novel noninvasive tool to assess tissue stiffness.[13] Malignant lesions tend to be harder than benign lesions; hence, elastography could be used in the differential diagnosis of a thyroid nodule. There are two main types of elastography currently in clinical use, strain elastography (SE), and shear wave elastography (SWE).[14] Both methods can be used to assess tissue stiffness and aid in the diagnosis of thyroid nodules. Only one study directly compared the diagnostic accuracies of SE and SWE simultaneously; the results were comparable between these two methods. However, a recent meta-analysis pooled individual studies of SE and SWE and found that SWE was superior to SE.[15] Therefore, there is no clear consensus regarding whether SE or SWE is the superior method.

It was hypothesized that the addition of elastography can increase the diagnostic performance beyond the conventional US mode.[16] To date, there has been no study to support the superiority of either combination of traditional US and novel elastography. The aims of this study were to compare SE, SWE, and traditional gray-scale US in assessing thyroid nodules.

Subjects and Methods

Patient recruitment

The study protocol was approved by the Institutional Ethical Review Board (105061-E). From July 2015 to July 2016, we prospectively recruited patients who underwent H and N US examination and US-FNA cytology of thyroid nodules after informed consents were obtained. No patient in this series had a previous diagnosis of thyroid malignancy. Patients with cytology results with Bethesda system ratings of II, V, and VI were enrolled for further analysis.

Conventional ultrasound

Two ultrasonologists with >5 years of experience in thyroid imaging and >2 years in US elastography performed all US examinations. The US equipment consisted of a Toshiba Aplio 500 US system (Otawara, Japan) with a 5–14 MHz L probe. All morphologic US parameters and vascular features were thoroughly evaluated and recorded on the PACS system (Marotech Inc., Seoul, South Korea) for the largest nodal lesion in each patient. The settings for Power Doppler sonography were set for high sensitivity with a low wall filter to allow for the detection of vessels with low blood flow. The color gain was increased gradually until background noise appeared and then decreased until the noise was suppressed, thus ensuring maximum sensitivity according to the Bude and Rubin description.[17]

Each thyroid nodule was first assessed with gray-scale sonography for morphologic parameters in the horizontal section. The AP diameter and TR diameter were measured. The echo structure was categorized as a predominantly solid component or mixed cyst. Echogenicity with respect to the surrounding soft tissue was assessed and classified as hypoechoic, isoechoic, or hyperechoic. The nodule margin was defined as regular or irregular. Microcalcification was distinguished as absent or present. Internal echotexture was divided into heterogeneity or homogeneity. Vascular patterns were then surveyed by Power Doppler sonography and categorized as a group of avascular or peripheral type versus that of the marked intranodular type. The former was classified as normal vascularization and the latter as abnormal vascular development.

Traditional prediction model

According to our previous publication,[12] the presence of microcalcification, a taller-than-wide shape, a predominant solid echostructure, and irregular margins have been shown to be good independent predictive parameters. We developed the following computerized scoring systems: score = 1.25 × margin (regular = 0; irregular = 1) + 2.03 × micro-calcification (absent = 0; present = 1) + 1.56 × echo-texture (mixed cystic and solid = 0; predominate solid = 1) + 1.76 × taller-than-wide shape (absent = 0; present = 1).[12] This scoring system is incorporated in our hospital US reporting system and freely shared on the website.[16] A thyroid nodule is classified as positive with a score ≥3.3

corresponding to sensitivity of 80.0%, specificity of 90.5%, PPV of 45.2%, NPV of 97.9%, and overall accuracy of 89.5%.

Shear wave elastography

In the SWE method that was developed by the manufacturer, part of the tissue was deformed by a "push pulse", the velocity of the shear waves propagating within the tissue was detected, and the stiffness of the tissue was assessed based on the detected shear velocity within the tissue. With this SWE method, light compression was applied over the skin with an US probe, and it was possible to observe whether the shear waves propagated properly through the tissue in a single still image displayed in propagation mode [arrival time contour, Figures 1 and 2a]. In areas where the contour lines were parallel, the shear waves propagated properly, and the reliability of the obtained data was high. We then shifted to Young's modules [kPa, Figures 1 and 2b]. The SWE image was displayed alongside the gray-scale US image (right side of the screen) for nodule localization. The representative region in the nodule was selected by visual inspection. The elastic mode of the stiffest regions in each node was measured on color-coded elastograms with Young's modulus values (mean SWE value and standard deviation [SD], kPa) shown within an approximately 5 mm circular region.

Strain elastography

During the SE procedure, images were also displayed superimposed and adjacent to the gray-scale US as a dual-panel image [Figures 1 and 2c]. Next, the sonographers followed light pressure compression with repeated decompression until nearly identical size and color distribution of the region of interest in several consecutive images was obtained. The strain quality indicator was determined by manual appropriate compression adjustments to obtain smooth sine waves and avoid under-or over-compression [left lower part in Figures 1 and 2c]. The sonographers also orientated the direction of compression along the radiation axis and avoided out-of-plane motion. The SE of each patient was performed by one operator. The SE pattern was assessed based on a color scale, with blue being correlated with hard tissue, red with soft tissue, and green with tissue of intermediate hardness. The nodules were classified into the following four elastography scoring (ES) system scores: ES I, a prevalence of red and green color; ES II, a prevalence of green in >50% of the nodule; ES III, a prevalence of blue in at least 50% of the nodule; and ES IV, a prevalence of blue in at least 75% of the nodule.[18,19] The elastograms were reviewed independently by two raters who had performed SE.

Ultrasound-guided fine-needle aspiration and cytology

US-FNA was conducted with the array probe guiding the placement of a 22G fine needle [Figures 1 and 2d, arrows revealed the needles on the screen]. Several passes in the lesion were made to obtain sufficient material for cytology assessment. Both sonography and US-FNA were performed

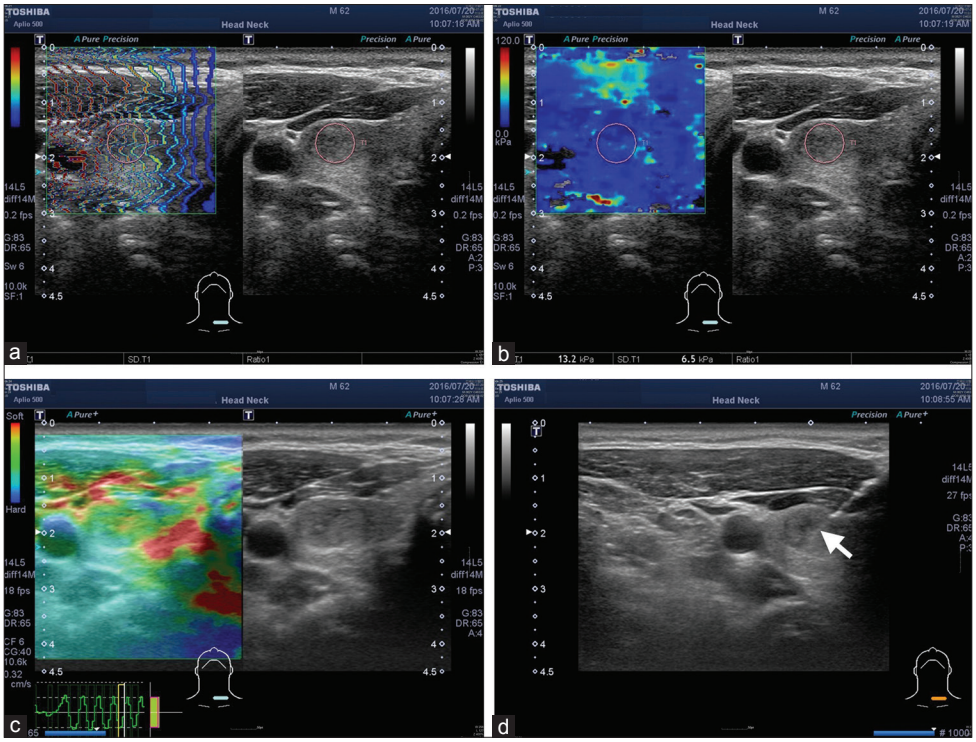

Figure 1: Representative case demonstration, a 62-year-old male with left side thyroid nodule. The size was measured as 1.53 cm. The shear waves propagated through the tissue in a single still image displayed in propagation mode (arrival time contour, a). The mean shear wave elastography value was 13.2 kPa with a standard deviation of 6.5 kPa (b). The strain elastography revealed elastographic scoring pattern 2 (c), and the tradition score was 1.56. Fine-needle aspiration was performed under the guidance of US (arrow, d). The final cytology showed that the nodule was Class II The Bethesda System for Reporting Thyroid Cytopathology and a benign thyroid nodule was diagnosed

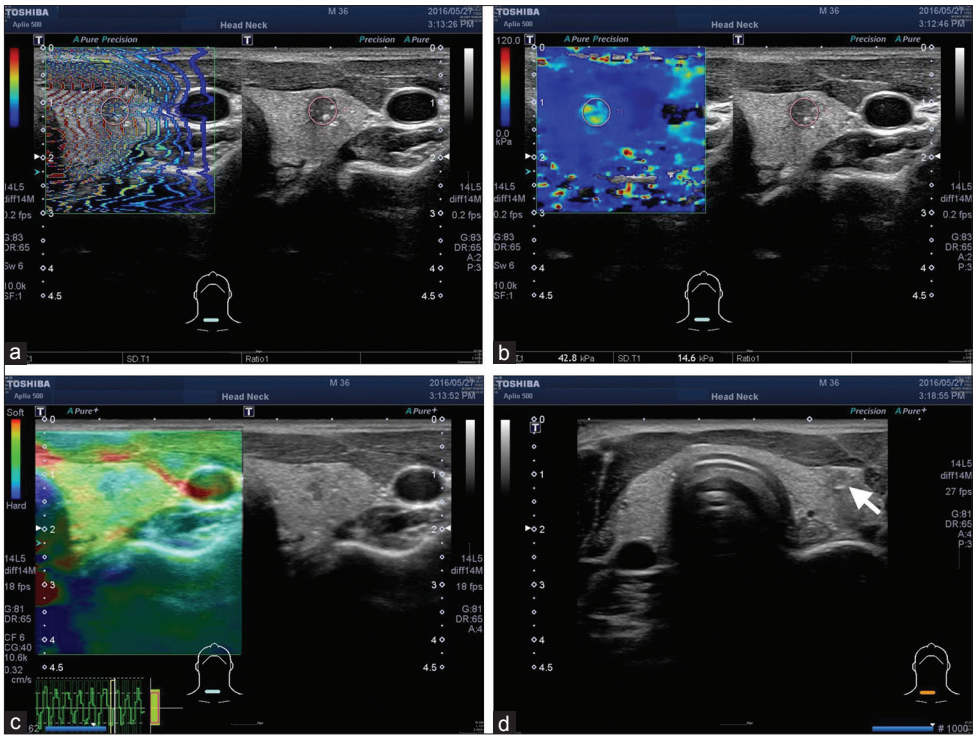

Figure 2: Another 36-year-old male with a right thyroid nodule. The size was measured as 0.85 cm. The shear waves propagated through the tissue, resulting in a single still image displayed in propagation mode (arrival time contour, a). The mean shear wave elastography value was 42.8 kPa with a standard deviation of 14.6 kPa (b). The strain elastography revealed elastographic scoring pattern 4 (c), and the tradition score was 4.84. fine-needle aspiration was performed under the guidance of US (arrow, d); the final cytology revealed the nodule was Class VI The Bethesda System for Reporting Thyroid Cytopathology, and a thyroid papillary carcinoma was diagnosed

by the same physician using standardized procedures as previously described.[12] Half of the four slides were air-dried for Liu's stain, and the other half were rapidly fixed in alcohol for the Papanicolaou stain. The cytological diagnoses were made in accordance with the six diagnostic categories of the TBSRTC,[6] namely: I indicated nondiagnostic or unsatisfactory analysis, II indicated a benign lesion, III indicated atypia or a follicular lesion, IV indicated follicular neoplasm or suspicion of a follicular neoplasm, V indicated a suspicion of malignancy, and VI indicated a malignant lesion. The cytology results with Bethesda system ratings of II, V, and VI were recruited for further analysis.

Statistical analysis

The conventional US characteristics, vascular features, SE, and SWE parameters were compared by Mann–Whitney test, Chi-square test, or Fisher's exact test, when appropriate. The optimal cutoff values of mean SWE values for predicting malignancy were determined with receiver operating characteristic (ROC) curve analysis. Univariate and multivariate logistic regression analysis was also performed; the odds ratio (OR) and 95% confidence interval (CI) were used to evaluate the association of those parameters with malignancy. Backward selection procedures with 0.1 levels for staying in the prediction model were used to construct an extended model with elastography parameters. Diagnostic performances were calculated regarding sensitivity, specificity, PPV, NPV, and area under the curves (AUCs) (C-statistic). We compared the AUC of the extended model with elastography data to the traditional prediction score.[12] The statistical significance was set at $P < 0.05$. The statistical analyses were performed using STATA software, version 12.0 (STATA Statistical Software: Release 12. STATA Corp LP, College Station, TX, USA).

Results

From August 2015 to July 2016, 185 consecutive patients with thyroid nodules who underwent US-FNA and cytology indicating TBRCT class II, V, and VI were reviewed. Among them, 129 (70%) were female, and 56 (30%) were male; their age ranged from 20 to 84 years old (mean of 51 years old). Nearly 164 (89%) were classified as benign, and 21 (11%) were classified as malignant according to TBSRTC and final pathology. For the cytological results in categories IV to VI, surgical interventions for the thyroid nodules were performed. The final diagnosis of malignancy ($n = 21$) was made by pathologic results and all revealed papillary carcinoma. The nodules with cytological results in categories II were under regular US follow-up and those that did not increase in sonographic size were considered to be affected by benign processes during the follow-up period of at least 6 months.

Comparisons of demographic data and traditional US and elastography features are shown in Table 1. Benign and malignant nodules had different distributions of features

Table 1: Demographic data, ultrasound, and elastography characteristics of recruited patients with thyroid nodules

	Benign (n=164) TBSRTC (II)	Malignant (n=21) TBSRTC (V and VI)	*P*
Age	51.7±13.5	46.5±13.2	0.10
Gender (female:male)	117 (71%)/47 (29%)	12 (57%)/9 (43%)	0.18
Side (left:right)	84/80	7/14	0.12
Size (cm)	2.0±1.1	1.3±0.7	<0.01
Irregular boundary	96/68	6/15	0.01
Heterogeneous internal echo	97/67	9/12	0.16
Hypoechogenicity	33/131	0/21	0.02
Microcalcification	141/23	7/14	<0.01
Predominant solid architecture	57/107	3/18	0.06
Marked intranodular vascular pattern	88/74	8/13	0.16
Taller than wide shape	141/23	10/11	<0.01
Mean SWE value (kPa)	33.1±25.2	51.0±24.4	<0.01
SD SWE value (kPa)	19.8±14.1	29.3±13.2	<0.01
SE pattern (1 and 2/3 and 4)	114/50	4/17	<0.01
Score (<3.3/≥3.3)	133/31	3/18	<0.01

TBSRTC: The Bethesda System for Reporting Thyroid Cytopathology, SWE: Shear wave elastography, SD: Standard derivation, SE: Strain elastography

including size (2.0 ± 1.1 cm vs. 1.3 ± 0.7 cm, $P < 0.01$), an irregular boundary (68/164 [41%] vs. 15/21 [71%], $P < 0.01$), hypoechogenicity (131/164 [80%] vs. 21/21 [100%], $P < 0.01$), microcalcification (23/164 [14%] vs. 14/21 [67%], $P < 0.01$), a taller-than wide shape (23/164 [14%] vs. 11/21 [52%], $P < 0.011$), mean SWE value (33.1 ± 25.2 vs. 51.0 ± 24.4 kPa, $P < 0.01$), SD of SWE values (19.8 ± 14.1 vs. 29.3 ± 13.2 kPa, $P < 0.01$), SE patterns (ES patterns 3 and 4; 50/165 vs. 17/21, $P < 0.01$), and traditional prediction scores (31/164 [19%] vs. 18/21 [86%], $P < 0.01$). The significance of predominant solid echotexture was borderline (107/165 vs. 18/21, $P = 0.06$).

Further ROC analysis of mean SWE values revealed the optimal cutoff point was 32 kPa with a sensitivity of 81% (95% CI: 64%–98%) and a specificity of 65% (57%–72%). We further use this cutoff point in univariate logistic regression; the results are shown in Table 2. The SE pattern (ES patterns 3 and 4, OR: 9.7, 95% CI: 3.1–30.3) and mean SWE value (≥32 kPa; OR: 7.8; 2.5–24.2) were significant predictors for malignancy. The results of the multivariate logistic regression are shown in Table 3. After adjusting for size and four traditional US predictors (an irregular boundary, microcalcification, architecture, and a taller-than-wide shape), the mean SWE value (≥32 kPa) was still an independent predictor for malignancy (OR: 16.8, 3.6–78.3, $P < 0.01$).

The diagnostic performance of various US features, elastography parameters, and traditional score are summarized in Table 4. We found the diagnostic performances of SE (patterns 3 and 4) and SWE (≥32 kPa) were comparable in sensitivity (81% vs. 81%), specificity (70% vs. 65%), PPV (25% vs. 23%), and NPV (97 vs. 96%).

If we developed an extended elastography scoring model with stepwise selection under logistic regression, four predictors including micro-calcification, a taller-than-wide shape, and SE (patterns 3 and 4) and mean SWE values (≥32 kPa) were selected. The new extended model can be expressed as follows: 8.38 × microcalcification (absent = 0; present = 1) +4.91 × taller-than-wide shape (absent = 0; present = 1) +3.55 × strain elastography (patterns 1 and 2 = 0; patterns 3 and 4 = 1) + 12.06 × mean SWE value (<32 kPa = 0; ≥32 kPa = 1). With ROC curve analysis, the optimal cutoff point (≥15) comprised a sensitivity of 86%, a specificity of

Table 2: Results of univariate logistic regression analysis

Univariate analysis	OR	95% CI	*P*
Age (years)	1.0	0.9-1.0	0.10
Gender (female: male)	1.9	0.7-4.7	0.19
Size (cm)	0.3	0.1-0.7	<0.01
Irregular boundary	3.5	1.3-9.6	0.01
Heterogeneous internal echo	1.9	0.8-4.8	0.16
Microcalcification	12.3	4.5-33.6	<0.01
Predominant solid architecture	3.2	0.9-11.3	0.07
Tall than wide shape	6.7	2.6-17.7	<0.01
Mean SWE value (≥32 kPa)	7.8	2.5-24.2	<0.01
SE patterns (3 and 4)	9.7	3.1-30.3	<0.01

SWE: Shear wave elastography, SE: Strain elastography, OR: Odds ratio, CI: Confidence interval

Table 3: Results of multivariate logistic regression analysis

Malignancy	OR	95% CI	*P*
Size (cm)	0.5	0.2-1.5	0.21
Irregular boundary	0.8	0.2-3.3	0.70
Microcalcification	7.3	1.8-30.3	0.01
Predominant solid architecture	1.2	0.2-6.0	0.85
Taller than wide shape	4.3	1.1-17.1	0.04
Mean SWE value (≥32 kPa)	16.8	3.6-78.3	<0.01
SE patterns (3 and 4)	3.4	0.8-14.6	0.10

SWE: Shear wave elastography, SE: Strain elastography, OR: Odds ratio, CI: Confidence interval

Table 4: Comparison of the diagnostic performance of different ultrasonographic features and elastography

	Sensitivity (%)	95% CI	Specificity (%)	95% CI	PPV (%)	95% CI	NPV (%)	95% CI
Boundary (regular/irregular)	71	52-91	59	51-66	53	53-53	94	90-99
Internal echo (homo/heterogeneous)	57	36-78	59	52-67	15	7-23	92	86-97
Microcalcification (absent/present)	67	47-87	86	81-91	38	22-53	95	92-99
Architecture (cystic/solid)	86	71-101	35	27-42	14	8-21	95	89-101
Taller-than-wide	52	31-74	86	81-91	32	17-48	93	89-97
SE patterns (3 and 4)	81	64-98	70	62-77	25	15-36	97	93-100
Mean SWE value (≥32 kPa)	81	64-98	65	57-72	23	13-32	96	93-100
Tradition score* (≥3.3)	86	71-101	81	75-87	37	23-50	98	95-100
Extended model# (≥15)	86	71-100	82	76-88	38	24-52	98	95-100

*Tradition score = 1.25 × margin (regular = 0; irregular = 1) + 2.03 × micro-calcification (absent = 0; present = 1) + 1.56 × echo-texture (mixed cystic and solid = 0; predominate solid = 1) + 1.76 × taller-than-wide shape (absent = 0; present = 1). #Extended elastography model = 8.38 × micro-calcification (absent = 0; present = 1) + 4.91 × taller-than-wide shape (absent = 0; present = 1) + 3.55 × strain elastography (patterns 1 and 2 = 0; patterns 3 and 4 = 1) + 12.06 × mean SWE value (<32 kPa = 0; ≥32 kPa = 1). CI: Confidence interval, PPV: Positive predictive value, NPV: Negative predictive value, SWE: Shear wave elastography, SE: Strain elastography

81%, a PPV of 37%, and an NPV of 98%. The performance was comparable to traditional prediction scores[12] with a sensitivity of 86%, a specificity of 81%, a PPV of 36%, and an NPV of 98% [Table 4]. A comparison of the AUCs between the traditional model and extended model was also performed; the AUCs were 0.88 (0.81–0.94) and 0.91 (0.85–0.97), respectively. There was still no significant improvement in C-statistics ($P = 0.4$) [Figure 3].

Discussion

Various US features have been reported as predictors of malignancy in thyroid nodules. Our results also supported the concept of tissue stiffness that can be used in diagnosing malignancy. The malignancies tended to be harder in SE and SWE. Mean SWE was an independent predictor after multivariable regression. We noted a large SD of SWE in malignancy. We also developed an extended model combining two elastography methods and two traditional US features; unfortunately, the diagnostic performance was not significantly improved.

Before introduction to the new diagnostic parameters, it was necessary to compare the new modality to previously used diagnostic tools. Elastography has been thought to improve diagnostic performance in thyroid nodule diagnosis.[16] One previous report directly compared SE and SWE.[20] A total of 64 nodules were recruited with 19 malignancies and 45 benignities; their results revealed comparability in sensitivity, specificity, NPV, and PPV with a cutoff of mean SWE ≥38.3 kPa. One recent diagnostic meta-analysis collected SE and SWE data individually and showed that SE had a better diagnostic performance than SWE.[15] In our study, we recruited more thyroid nodules; however, SE and SWE also revealed comparable diagnostic performance under a head-to-head comparison; SE was not superior to SWE. Dobruch–Sobczak *et al*. compared SWE and conventional B-mode parameters with 169 thyroid nodules; they concluded that a combination of SWE and conventional B-mode parameters does not improve diagnostic performance.[21]

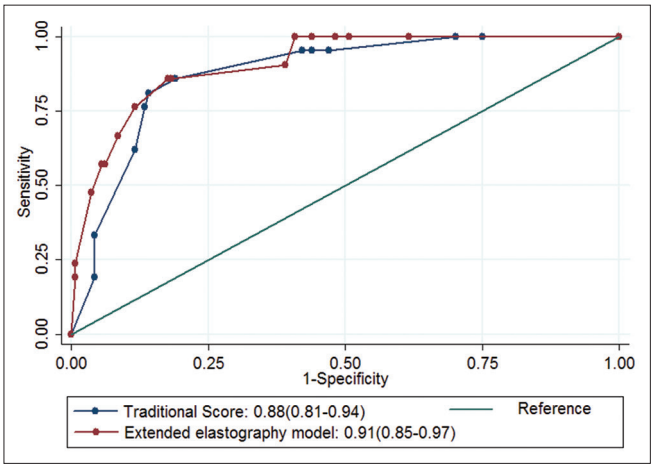

Figure 3: We used stepwise logistic regression to keep predictors at a 0.1 significant level. Two B mode features (microcalcification and a taller-than-wide shape) and two elastography features (mean shear wave elastography [≥32 kPa] and strain elastography [elastographic scoring patterns 3 and 4]) were used to construct the extended model. The area under the curves of the previous score and extended elastography model were compared; the area under the curves were 0.88 (95% confidence interval: 0.81–0.94) and 0.91 (95% confidence interval: 0.85–0.97) for the traditional model and extended elastography model, respectively. Statistically, there was no significant improvement in area under the curves between these two models ($P = 0.40$)

The novelty of this study is that we developed a new prediction model that adapted both SE and SWE features according to a logistic regression model. We used stepwise logistic regression to select predictors with a 0.1 significance level. Two B-mode features (microcalcification and a taller-than-wide shape) and two elastography features (mean SWE [≥32 kPa] and SE [patterns 3 and 4]) were used to construct an extended model under logistic regression analysis. The AUC was 0.91 (95% CI: 0.85–0.97) for extended elastography data. There was no significant improvement in AUC compared to the traditional US model. The AUC was 0.88 (95% CI: 0.81–0.94, $P = 0.40$). Detailed results of the diagnostic performances are shown in Table 4 and Figure 3. Compared to the previous

traditional model,[12] the new extended model did not improve the diagnostic performance. Our results were comparable to previous reports.[22]

In this study, we also validated a previous prediction B mode model with a sensitivity of 86%, a specificity of 81%, a PPV of 37%, an NPV of 98%, and an AUC of 0.88 (0.81–0.94). With four traditional B-mode parameters, the prediction rule had good diagnostic performance. Therefore, basic B-mode parameters are still fundamental in the diagnosis of thyroid malignancy.

According to some previous reports, tumor heterogeneity is ever reported, and the SD of SWE is an indicator of tissue heterogeneity. Some recent reports assessed tissue texture analysis and showed good diagnostic performance.[22] We also noted a larger SD of mean SWE values for malignancy [Table 1]. According to other previous reports, tumor heterogeneity is reported for malignancy, and the SD of SWE is an indicator of tissue heterogeneity. Most recent reports assessed tissue texture analysis and showed good diagnostic performance.[22] However, the analysis of tissue heterogeneity requires off-line analysis and real-time analysis is not available.

There are some limitations to this study. First, some previous reports used maximum SWE values to predict malignancy; however, our machine does not offer these data. Second, according to previous reports, the compression level can influence the diagnostic performance, but we did not use multiple compression levels. Third, the case numbers were still limited and mainly depended on papillary carcinoma.

Conclusion

Our findings support elastography as an independent factor in diagnosing thyroid cancer. However, in comparing the new extended elastography model to our previous prediction model, the new extended model showed no significant difference in diagnostic performance. Further study is necessary to explore the utility of elastography in thyroid nodule assessment in a clinical setting.

Acknowledgment

This work was supported by grants from the Far Eastern Memorial Hospital and Yuan Ze University Joint Research Program (FEMH-YZU-2016-007).

Financial support and sponsorship

Nil.

Conflicts of interest

There are no conflicts of interest.

References

1. Brander A, Viikinkoski P, Nickels J, Kivisaari L. Thyroid gland: US screening in a random adult population. Radiology 1991;181:683-7.
2. Tan GH, Gharib H. Thyroid incidentalomas: Management approaches to nonpalpable nodules discovered incidentally on thyroid imaging. Ann Intern Med 1997;126:226-31.
3. Wang C, Crapo LM. The epidemiology of thyroid disease and implications for screening. Endocrinol Metab Clin North Am 1997;26:189-218.
4. Nam-Goong IS, Kim HY, Gong G, Lee HK, Hong SJ, Kim WB, *et al.* Ultrasonography-guided fine-needle aspiration of thyroid incidentaloma: Correlation with pathological findings. Clin Endocrinol (Oxf) 2004;60:21-8.
5. Gallo M, Pesenti M, Valcavi R. Ultrasound thyroid nodule measurements: The "gold standard" and its limitations in clinical decision making. Endocr Pract 2003;9:194-9.
6. Cibas ES, Ali SZ; NCI Thyroid FNA State of the Science Conference. The bethesda system for reporting thyroid cytopathology. Am J Clin Pathol 2009;132:658-65.
7. Shimura H, Haraguchi K, Hiejima Y, Fukunari N, Fujimoto Y, Katagiri M, *et al.* Distinct diagnostic criteria for ultrasonographic examination of papillary thyroid carcinoma: A multicenter study. Thyroid 2005;15:251-8.
8. Cappelli C, Castellano M, Pirola I, Cumetti D, Agosti B, Gandossi E, *et al.* The predictive value of ultrasound findings in the management of thyroid nodules. QJM 2007;100:29-35.
9. Kim EK, Park CS, Chung WY, Oh KK, Kim DI, Lee JT, *et al.* New sonographic criteria for recommending fine-needle aspiration biopsy of nonpalpable solid nodules of the thyroid. AJR Am J Roentgenol 2002;178:687-91.
10. Moon WJ, Jung SL, Lee JH, Na DG, Baek JH, Lee YH, *et al.* Benign and malignant thyroid nodules: US differentiation – Multicenter retrospective study. Radiology 2008;247:762-70.
11. Neeman T. Clinical prediction models: A practical approach to development, validation, and updating by Ewout W. Steyerberg. Int Stat Rev. 2009;77:320-1.
12. Cheng PW, Chou HW, Wang CT, Lo WC, Liao LJ. Evaluation and development of a real-time predictive model for ultrasound investigation of malignant thyroid nodules. Eur Arch Otorhinolaryngol 2014;271:1199-206.
13. Hong Y, Liu X, Li Z, Zhang X, Chen M, Luo Z, *et al.* Real-time ultrasound elastography in the differential diagnosis of benign and malignant thyroid nodules. J Ultrasound Med 2009;28:861-7.
14. Shiina T, Nightingale KR, Palmeri ML, Hall TJ, Bamber JC, Barr RG, *et al.* WFUMB guidelines and recommendations for clinical use of ultrasound elastography: Part 1: Basic principles and terminology. Ultrasound Med Biol 2015;41:1126-47.
15. Tian W, Hao S, Gao B, Jiang Y, Zhang S, Guo L, *et al.* Comparison of diagnostic accuracy of real-time elastography and shear wave elastography in differentiation malignant from benign thyroid nodules. Medicine (Baltimore) 2015;94:e2312.
16. Magri F, Chytiris S, Chiovato L. The role of elastography in thyroid ultrasonography. Curr Opin Endocrinol Diabetes Obes 2016;23:416-22.
17. Bude RO, Rubin JM. Power Doppler sonography. Radiology 1996;200:21-3.
18. Rago T, Vitti P. Role of thyroid ultrasound in the diagnostic evaluation of thyroid nodules. Best Pract Res Clin Endocrinol Metab 2008;22:913-28.
19. Rago T, Vitti P. Potential value of elastosonography in the diagnosis of malignancy in thyroid nodules. Q J Nucl Med Mol Imaging 2009;53:455-64.
20. Liu BX, Xie XY, Liang JY, Zheng YL, Huang GL, Zhou LY, *et al.* Shear wave elastography versus real-time elastography on evaluation thyroid nodules: A preliminary study. Eur J Radiol 2014;83:1135-43.
21. Dobruch-Sobczak K, Zalewska EB, Gumińska A, Słapa RZ, Mlosek K, Wareluk P, *et al.* Diagnostic performance of shear wave elastography parameters alone and in combination with conventional B-mode ultrasound parameters for the characterization of thyroid nodules: A prospective, dual-center study. Ultrasound Med Biol 2016;42:2803-11.
22. Bhatia KS, Lam AC, Pang SW, Wang D, Ahuja AT. Feasibility study of texture analysis using ultrasound shear wave elastography to predict malignancy in thyroid nodules. Ultrasound Med Biol 2016;42:1671-80.